Environmental Science
Processes & Impacts

Limitations of conventional approaches to identify photochemically produced reactive intermediates involved in contaminant indirect photodegradation

Journal:	*Environmental Science: Processes & Impacts*
Manuscript ID	EM-ART-07-2023-000304.R1
Article Type:	Paper

Environmental Significance Statement

Indirect photodegradation is an important pathway for the degradation of many aquatic contaminants. Quenching experiments are often used to evaluate the importance of photochemically produced reactive intermediates (PPRI) in the degradation of contaminants. By performing quenching experiments on four contaminants in a wide range of waters, we highlight the potential problems inherent in quenching experiments due to the lack of selectivity of quenching compounds and the complex interrelated nature of different PPRI. We also perform regression analysis to relate PPRI formation with the degradation of aquatic contaminants as an alternative to quenching experiments.

Limitations of conventional approaches to identify photochemically produced reactive intermediates involved in contaminant indirect photodegradation

*Reid P. Milstead[1], Stephanie M. Berg[1], Bella M. Kelly[2], Christian D. Knellwolf[2], Cooper J. Larson[2], Kristine H. Wammer[2], and Christina K. Remucal[1,3]**

[1]Environmental Chemistry and Technology Program
University of Wisconsin – Madison
Madison, Wisconsin 53706

[2]Department of Chemistry
University of St. Thomas
St. Paul, Minnesota 55105

[3]Department of Civil and Environmental Engineering
University of Wisconsin – Madison
Madison, Wisconsin 53706

*Corresponding author address: 660 N. Park St., Madison, WI 53706;
email: remucal@wisc.edu; telephone: (608) 262-1820; fax: (608) 262-0454; Twitter: @remucal

Abstract

Dissolved organic matter (DOM) mediated indirect photodegradation can play an important role in the degradation of aquatic contaminants. Predicting the rate of this process requires knowledge of the photochemically produced reactive intermediates (PPRI) that react with the compound of interest, as well as the ability of individual DOM samples to produce PPRI. Key PPRI are typically identified using quencher studies, yet this approach often leads to results that are difficult to interpret. In this work, we analyze the indirect photodegradation of atorvastatin, carbamazepine, sulfadiazine, and benzotriazole using a diverse set of 48 waters from natural and engineered aquatic systems. We use this large data set to evaluate relationships between PPRI formation and indirect photodegradation rate constants, which are directly compared to results using standard quenching experiments. These data demonstrate that triplet state DOM (^{3}DOM) and singlet oxygen ($^1O_2$) are critical PPRI for atorvastatin, carbamazepine, and sulfadiazine, while hydroxyl radical ($^{\bullet}$OH) contributes to the indirect photodegradation of benzotriazole. We caution against relying on quenching studies because quenching of ^{3}DOM limits the formation of $^1O_2$ and all studied quenchers react with $^{\bullet}$OH. Furthermore, we show that DOM composition directly influences indirect photodegradation and that low molecular weight, microbial-like DOM is positively correlated with the indirect photodegradation rates of carbamazepine, sulfadiazine, and benzotriazole.

Introduction

Photodegradation can play a major role in the fate of polar organic compounds, including pesticides and pharmaceuticals, in surface waters. Some compounds primarily degrade through direct absorption of light via direct photodegradation.[1–5] The presence of dissolved organic matter (DOM) can lead to enhanced photodegradation of other compounds, particularly those that are not effective at absorbing the wavelengths associated with natural sunlight.[1,3,6–12] During indirect photodegradation, DOM, rather than the contaminant, absorbs light and is promoted to an excited state that can lead to the production of photochemically produced reactive intermediates (PPRIs), including triplet state DOM (^{3}DOM), singlet oxygen ($^1O_2$), hydroxyl radical ($^{\bullet}$OH), and other radical species.[13–17] These reactive species may then react with the target compound. Photodegradation, whether direct or indirect, can be more efficient than other natural loss processes (e.g., biodegradation and sorption) for many classes of pesticides and pharmaceuticals.[9,18]

DOM is a highly diverse, heterogenous mixture of organic compounds derived from plant and microbial residues that is found in all waters. The concentration and composition of DOM varies widely in the environment. For example, concentrations range from 1 – 3 mg-C L^{-1} in oligotrophic systems to 10 – >35 mg-C L^{-1} in rivers and wetlands.[19–25] The composition of DOM is determined by its source (e.g., terrestrial and/or microbial) and its extent of biological and photochemical processing. Importantly, the composition of DOM plays a major role in the formation of PPRI. For example, microbial-like DOM, which is often lower in molecular weight and more aliphatic in nature, is often more efficient at producing ^{3}DOM and $^1O_2$.[26–36] In contrast, $^{\bullet}$OH production is more strongly associated with aromatic DOM.[24,37]

Understanding the persistence of pharmaceuticals, pesticides, and other trace contaminants commonly found in water systems is important because many of these compounds can have adverse impacts on human and ecosystem health. For example, the pharmaceuticals atorvastatin, carbamazepine, and sulfadiazine are biologically active at low concentrations,[38] making environmentally relevant concentrations a potential concern. Similarly, benzotriazole is used in industrial processes as a corrosion inhibitor[39] and is difficult to remove during wastewater treatment.[40] While the mode of benzotriazole toxicity is less well understood, it can have negative impacts on aquatic organisms and plants at environmentally relevant concentrations.[41,42]

It is challenging to predict indirect photodegradation rates because compounds react differently with individual PPRI and because PPRI formation efficiencies vary widely among DOM samples. Therefore, identifying the PPRI responsible for contaminant indirect photodegradation is a major focus in better understanding contaminant fate. PPRI identification is most commonly achieved through quencher experiments in which a "PPRI-specific" quencher is added to solution and a change in reaction rate is interpreted as evidence of PPRI involvement.[1,3] This simple approach can be used on small sample sets, but is prone to biases because quenchers can impact non-target PPRI formation (e.g., ^{3}DOM quenchers react with $^{\bullet}$OH). In larger data sets, correlations between PPRI formation and indirect photodegradation rates can serve as an alternate approach for identifying key PPRI. However, this approach has not yet been tested in a wide range of DOM sources or compared directly with the results of more standard quencher experiments.

In this study, we explore the indirect photodegradation of four aquatic contaminants (i.e., atorvastatin, benzotriazole, carbamazepine, and sulfadiazine) to identify the PPRI involved in their degradation and to establish relationships between DOM composition, contaminant degradation, and PPRI formation. To do this, we use DOM samples from both natural and engineered systems,

including 13 lake waters, 20 river waters, two agricultural ditches, and 13 wastewater samples, that range widely in DOM concentration and DOM composition as determined using bulk scale analyses and high-resolution mass spectrometry. We use this large data set to evaluate relationships between PPRI formation and indirect photodegradation rate constants, which are directly compared to results using standard quenching experiments. Finally, we evaluate the roles of DOM concentration and composition in indirect photodegradation. In addition to providing a better understanding of the indirect photodegradation of the four target compounds, the results have broader implications for the design and interpretation of contaminant quencher studies.

Materials and Methods

Materials. All chemicals were used as received. Additional details are provided in Electronic Supplementary Information **Section S1**.

Sample collection. Water samples (n = 48) were collected from five different geographical regions in Wisconsin and Minnesota, USA between August 2018 and September 2020. Samples include 13 lakes of differing trophic status, two agricultural ditches, and 20 river waters. Additionally, 13 wastewater samples were collected from four water treatment facilities (**Table S1**). More information about sample locations and collection can be found **Section S2**.[37]

Bulk water chemistry. The pH of all water samples was measured using a Mettler Toledo EL20 meter (**Table S2**), which was calibrated with standards obtained from Aqua Solutions (precision: ±0.1). Dissolved organic carbon (DOC) concentrations were quantified using a Shimadzu total organic carbon (TOC) analyzer (**Table S2**), which was calibrated using standards made from potassium hydrogen phthalate. Nitrate and nitrite were quantified using anion exchange chromatography (IC) using a Dionex ICS-2100 ion chromatography system with a Dionex IonPac

AS11-HC RFIC column (4 x 250 mm). Dissolved iron was quantified with inductively coupled plasma-optical emission spectroscopy (ICP-OES) using an Agilent 5110 VDV instrument (**Table S2**).

UV-visible (UV-vis) and fluorescence spectra of DOM were collected with a Horiba Aqualog Fluorimeter, which was capable of measuring both absorbance and fluorescence. Specific absorbance at 254 nm ($SUVA_{254}$) and E_2:E_3 (i.e., the ratio of absorbance at 250 nm to 365 nm) were used as proxies for average aromaticity and average molecular weight, respectively, as described previously (**Table S3**).[27,43,44] These values were corrected for nitrate absorbance, which resulted in changes of ~2%.[37] Fluorescence data were corrected for inner filter effects and Rayleigh scattering. The fluorescence index (FI) was calculated as the ratio of emission intensities at 470 nm and 520 nm upon excitation at 370 nm.[45] The humification index (HIX) was calculated as the sum of emissions from 435 – 480 nm divided by the sums of emission from 300 – 345 and 435 – 480 nm upon excitation at 254 nm.[46] Electron donating capacity was quantified using the 2,2'-azino-bis(3-ehtylbenzothiazoline-6-sulfonate) radical cation ($ABTS^{\bullet+}$) as described previously (**Table S3**).[37,47]

High-resolution mass spectrometry. DOM from each water sample was extracted via solid-phase extraction and eluted in methanol as described previously.[25,37,48] Extracts were diluted in 50:50 acetonitrile:water and directly injected into a Bruker FT-ICR MS (Solarix XR 12T) using negative mode electrospray ionization. Signals were exported, linearly calibrated, and compared with potential chemical formulas containing combinations of $^{13}C_{0-1}{}^{12}C_{5-80}H_{0-120}O_{0-80}N_{0-3}S_{0-1}$. Matches were required to meet a mass error cutoff threshold of <0.2 ppm and be part of a homologous series (+ CH_2 or CH_4 versus O).[24,49] Average weighted hydrogen to carbon ratios

(H:C_w), oxygen to carbon ratios (O:C_w), and double bond equivalents (DBE_w) were calculated for each sample based on formula matches (**Table S4**).

PPRI quantification. Samples were irradiated in a Rayonet photoreactor using sixteen 365 nm bulbs (full width half max = ±10 nm) to quantify PPRI formation. This wavelength range is within the solar spectrum[50] and allowed us to isolate DOM photolysis by minimizing nitrate absorbance.[37] Quantum yields and steady-state concentrations of $^1O_2$ and $^{\bullet}OH$ were quantified in undiluted samples using 10 μM furfuryl alcohol (FFA) and 10 μM terephthalic acid (TPA) as probe compounds, respectively (**Table S5**), as described previously.[24,51–53] TPA captures free $^{\bullet}OH$ and other hydroxylating species;[54] we refer to the combination as $^{\bullet}OH$ for simplicity. Quantum yield coefficients (f_{TMP}) for ^{3}DOM were quantified with 10 μM 2,4,6-trimethylphenol (TMP) as a probe compound using samples that were diluted to <5 mg-C L^{-1} due to the potential quenching effect of DOM on the radical cation intermediate of TMP as described previously.[28,55] Steady-state concentrations of ^{3}DOM were determined by dividing k_{obs} for the degradation of TMP by the second order rate constant for the reaction between TMP and ^{3}DOM (**Table S6**).[55,56] All samples were run in triplicate alongside a *p*-nitroanisole/pyridine actinometer to quantify light intensity.[57] The probes and actinometer were quantified by high performance liquid chromatography (HPLC). Details on calculations and quantification methods are provided in **Section S5**.

Contaminant degradation kinetics and quenching experiments. Atorvastatin, benzotriazole, carbamazepine, and sulfadiazine were separately added to filtered whole water samples to achieve concentrations of 10 μM and irradiated at 365 nm. Samples were collected at four time points and analyzed via HPLC to quantify degradation of each analyte (**Table S7**). Direct photodegradation controls were conducted by irradiating each analyte (10 μM) in buffered ultrapure water (30 mM borate; pH = 7.7 ± 0.1) and fit to first-order kinetics to calculate the direct

rate constant (k_{direct}). Borate was used as a buffer because precipitation was noted in some samples in the presence of phosphate. Observed rate constants (k_{obs}) were calculated in samples with DOM assuming pseudo-first-order kinetics. The k_{direct} and k_{obs} values were corrected for the impact of light screening.[58] Indirect photodegradation rate constants ($k_{indirect}$) were calculated as the difference between k_{obs} and k_{direct}. In the 15 out of the 192 possible contaminant/DOM pairs where k_{obs} was less than k_{direct}, $k_{indirect}$ is denoted as zero (**Table S8**). Carbon-normalized rate constants (k_C) were calculated by dividing $k_{indirect}$ by the dissolved organic carbon concentration of each sample (**Table S9**). More information on kinetics experiments and HPLC methods is provided in **Section S6**.

Additional contaminant photodegradation experiments were conducted using quenchers to indirectly investigate the role of PPRI in indirect photodegradation in select samples. Potassium sorbate was used to quench ^{3}DOM. Either histidine (atorvastatin) or DABCO (carbamazepine, sulfadiazine, benzotriazole) was used to quench $^1O_2$; the quencher was selected to avoid coelution with the target compound and/or transformation products. Isopropanol was used to quench radical species including $^{\bullet}$OH. Quenchers were added to water samples to achieve a concentration of 3 mM, which is similar to quencher concentrations used in past studies.[1,3,59,60] Additional experiments were conducted under anoxic conditions to further evaluate ^{3}DOM reactivity because removing oxygen increases the lifetime of this PPRI.[1,61] Samples were sparged with nitrogen gas for >8 minutes and irradiated in sacrificial capped vials with no headspace. Samples with quenchers and sparged samples were irradiated as described for the kinetics experiments (**Section S7**).

Statistical analysis. All PPRI and contaminant experiments were conducted in triplicate and error bars represent the standard deviation of these measurements. Linear regression analysis

was performed to relate rate constants of contaminant degradation to water chemistry, DOM composition, and PPRI formation. Indirect rate constants were correlated with [DOC], $[^1O_2]_{ss}$, $[^{\bullet}OH]_{ss}$, and $[^3DOM]_{ss}$. Carbon-normalized indirect rate constants were correlated with $SUVA_{254}$, E_2:E_3, HIX, FI, EDC, f_{TMP}, H:C_w, O:C_w, DBE_w, Φ_{1O2}, and Φ_{OH} because these values are also independent of [DOC] (**Section S8**).

Results and Discussion

DOM composition and photoreactivity. The photodegradation of the four target contaminants is quantified in 48 samples from natural and engineered systems to investigate how DOM composition impacts indirect photodegradation. Water types, DOM composition, and PPRI formation for these samples are summarized briefly here and are described in more detail in our previous work.[37] The natural waters used in this study vary widely in terms of water type, size, and location. We include 13 lakes of varying trophic statuses (i.e., oligotrophic, eutrophic, dystrophic, and mesotrophic), 20 river waters, and two agricultural ditches. For data visualization and discussion, the natural water samples are grouped according to geographical regions: St. Louis River (SLR), Northern Lakes, Yahara, Mankato, and Twin Cities (**Table S1**). Wastewater samples (n = 13) are grouped separately.

The concentration and composition of DOM varies widely in the water samples. [DOC] ranges from 1.8 to 69 mg-C L^{-1}, with high values observed in terrestrially impacted waters and lower values observed in oligotrophic lakes (**Table S2**). Optical properties derived from UV-vis and fluorescence spectroscopy, as well as data collected by high-resolution mass spectrometry, demonstrate that the composition of DOM is highly variable. For example, $SUVA_{254}$, which is related to measurements of aromaticity,[27,62] ranges from 0.2 to 4.79 L mg-C^{-1} m^{-1} (**Table S3**).

Similarly, E_2:E_3 is inversely related to direct measurements of molecular weight[43,62] and ranges from 4.93 to 13.03 (**Table S3**). Fluorescence indices such as FI and HIX range from 0.21 to 3.18 and 1.43 to 2.09, respectively (**Table S3**). Electron donating capacity (EDC), which is correlated with the concentration of redox active groups such as phenols,[47,63,64] ranges from 0.24 to 5.38 mmol e^- mg-C^{-1} L^{-1} (**Table S3**). An average of 4,026 ± 793 formulas are determined by FT-ICR MS. H:C_w ranges from 1.09 to 1.60 and is higher in wastewater and urban samples compared to rural or agricultural samples, which corresponds to more aliphatic DOM (**Table S4**). O:C_w ranges from 0.20 to 0.55 and is lower in urban samples than in other groups, which corresponds to more reduced DOM. Note that DOM composition can vary temporally and spatially within individual water bodies;[21,22,65,66] therefore, these samples represent DOM composition at the time of sample collection. Collectively, the bulk and molecular measurements demonstrate that the DOM composition in these samples spans the range expected in natural and engineered systems, making the results of this study applicable to many water systems.[37]

The photochemical production of ^{3}DOM, $^1O_2$, and $^{\bullet}$OH also ranges widely in these diverse samples, which is expected because the composition of DOM influences its photoreactivity.[21,24,25,37] The quantum yield coefficient of ^{3}DOM (f_{TMP}) ranges from 11.6 – 87.1 M^{-1} (average = 36.1 ± 17.9 M^{-1}) and the quantum yield of $^1O_2$ ranges from (0.6 – 8.27) x 10^{-2} (average = (3.4 ± 1.9) x 10^{-2}; **Table S6**). These parameters are highly correlated with each other[37] and the highest values are observed in urban and wastewater-impacted samples. The quantum yield of $^{\bullet}$OH ranges from (0.34 – 105) x 10^{-5} (average = 15 ± 23 x 10^{-5}; **Table S6**) and is not significantly correlated with f_{TMP} or Φ_{1O2}.[37] Measured steady-state concentrations range (5.8 – 122) x 10^{-15} M for ^{3}DOM, (0.4 – 12.6) x 10^{-13} M for $^1O_2$, and (0.57 – 32.5) x 10^{-16} M for $^{\bullet}$OH. $[^1O_2]_{ss}$ is positively correlated with $[^{\bullet}OH]_{ss}$, but neither are significantly correlated with $[^3DOM]_{ss}$ (**Figure S1**). Note

that the reported $[^3DOM]_{ss}$ values are an approximation because they assume a single, constant bimolecular reaction rate between ^3DOM and TMP; they are included here to facilitate linear regression analysis with indirect photodegradation rates. Also note that the production of $^{\bullet}OH$ is primarily attributable to DOM photolysis. Iron and nitrite concentrations are low (**Table S2**) and the photolysis of nitrate is negligible under this irradiation source.[37] The wide range of PPRI production quantum yields and steady-state concentrations are ideal for investigating the role of PPRI in the indirect photodegradation of the target compounds.

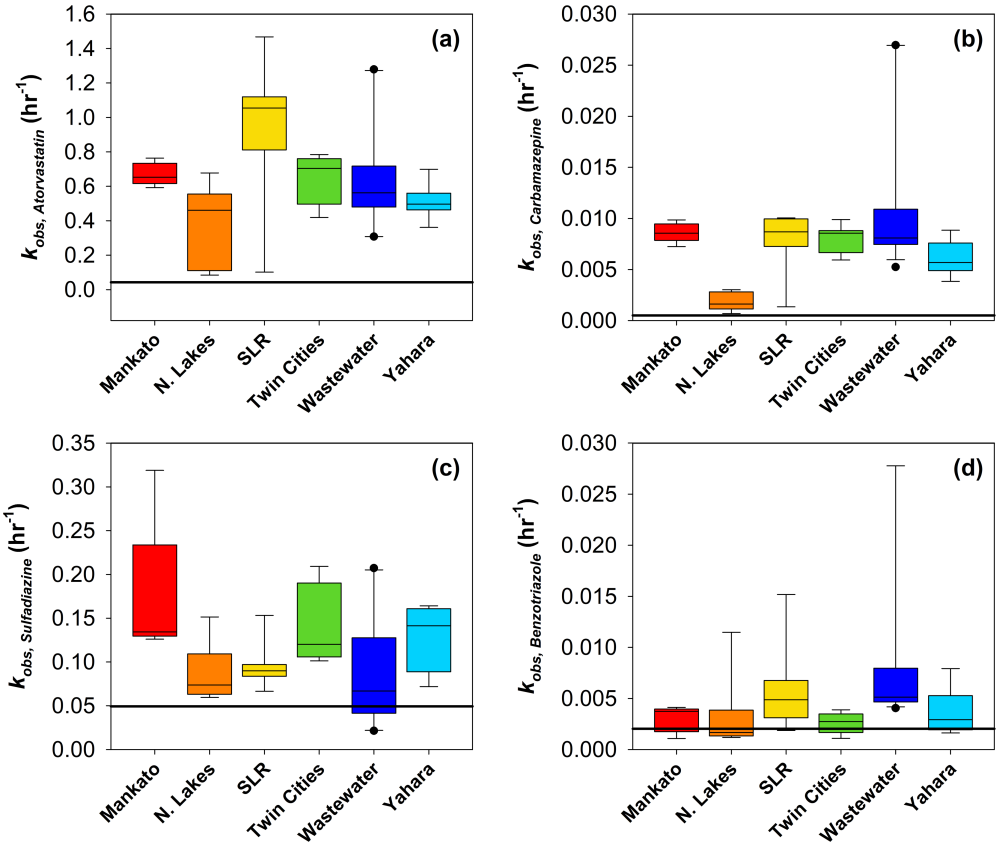

Figure 1. Observed rate constants (k_{obs}) for (a) atorvastatin, (b) carbamazepine, (c) sulfadiazine, and (d) benzotriazole in the 48 water samples collected from Mankato (n = 5), Northern Lakes (N. Lakes; n = 7), St. Louis River (SLR; n = 7), Twin Cities (n = 8), wastewater (n = 13) and the Yahara watershed (n = 8). Lines in the box-and-whisker plots represent the first and third quartiles. The line within each box represents the median. Whiskers represent minimum and maximum concentrations. Solid points represent outliers (i.e., any point less than the lower quartile or greater than the upper quartile by more than 1.5 times the interquartile range). The direct photodegradation rate constant (k_{direct}) is indicated with the solid black line.

Susceptibility of target compounds to direct and indirect photodegradation. The four target compounds (**Figure S2**) are separately irradiated in buffered ultrapure water and in the presence of DOM to investigate the importance of indirect photodegradation. All four compounds undergo direct photodegradation with first-order photodegradation rate constants (k_{direct}) of (5.1 ± 2.1) x 10^{-4} hr^{-1}, (2.0 ± 0.9) x 10^{-3} hr^{-1}, (5.0 ± 0.3) x 10^{-2} hr^{-1}, and (4.3 ± 2.1) x 10^{-2} hr^{-1} for carbamazepine, benzotriazole, sulfadiazine, and atorvastatin, respectively. In nearly all cases, the observed degradation rates are faster in the presence of DOM, demonstrating that the four compounds are susceptible to DOM-mediated indirect photodegradation (**Figure 1**). The k_{obs} values are 15.1 ± 11.5, 2.5 ± 2.9, 2.3 ± 1.1, and 14.7 ± 9.9 times faster on average in the presence of DOM for carbamazepine, benzotriazole, sulfadiazine, and atorvastatin, respectively (**Table S8**). Note that these reported rate constants are measured under laboratory conditions with a narrowband light source. Slower photodegradation is expected in the field due solar light intensity, light attenuation within the water column, and other environmental factors as described previously.[4,67–69]

The extent of indirect photodegradation varies widely depending on the target compound and the source of DOM. When considering natural water samples, the highest k_{obs} values of atorvastatin and benzotriazole are observed in samples from the St. Louis River watershed (**Figure 1**). In contrast, the highest observed photodegradation rate constants of carbamazepine and sulfadiazine are quantified in samples from Mankato. In general, DOM from the Northern Highlands of Wisconsin results in lower k_{obs} values for all compounds, which is interesting given that there is a wide range of DOM composition and concentration in these seven lakes (**Tables S1 – S3**). A wide range of k_{obs} values is observed when the target compounds are irradiated in the presence of DOM from the 13 wastewater effluent samples. For example, k_{obs} varies by a factor of

>15 for sulfadiazine and atorvastatin and >30 for carbamazepine and benzotriazole (**Figure 1**). The high variability in k_{obs} values for each compound indicates that DOM concentration and/or composition influences their indirect photodegradation rates.

While the photodegradation of atorvastatin and carbamazepine is faster in the presence of DOM in all 48 samples, there are exceptions for benzotriazole and sulfadiazine. The observed degradation rate is slower than k_{direct} in eleven cases for benzotriazole (Allequash Lake (N3), Big Muskellunge Lake (N4), Crystal Lake (N5), Sparkling Lake (N6), Trout Lake (N7), Wammer Ditch (M3), Lake Mendota (Y2), Confluence (Y8), Wisconsin Point (S7), Lake of the Isles (T6), and Lake Phalen (T8)) and in four cases for sulfadiazine (WLSSD Influent (W6) and Effluent (W7), Eagles Point Pre-UV (W12) and Post-UV (W13); **Table S8**). Over half of the waters where this occurred for benzotriazole are oligotrophic lakes which are similar in DOM concentration and composition, with low [DOC] (<5 mg-C L^{-1}), low $SUVA_{254}$ (<1.3 L mg-C^{-1} m^{-1}), high E_2:E_3 (>8.6), and low EDC (<0.76 $mmol_e^-$ mg-C^{-1} L^{-1}; **Tables S1 – S3**) and the only cases for sulfadiazine are wastewaters. Thus, DOM composition likely plays a role in the decreases seen in k_{obs} for this small number of contaminant/DOM pairs (i.e., 15 out of 192 experiments).

The role of DOM concentration compared to DOM composition is first assessed by calculating carbon-normalized rate constants (k_C; **Figure S3**). The k_C values range over approximately two orders of magnitude for atorvastatin ((0.5 to 12.2) x 10^{-2} hr^{-1} mg-C^{-1}), carbamazepine ((0.4 to 17.9) x 10^{-4} hr^{-1} mg-C^{-1}), sulfadiazine ((0.2 to 50.4) x 10^{-3} hr^{-1} mg-C^{-1}) and benzotriazole ((0.1 to 37.7) x 10^{-4} hr^{-1} mg-C^{-1}; **Table S9**). There are consistent trends across several of the water types. With the exception of benzotriazole, the fastest k_C values are observed in samples from Mankato (rural/agricultural). Samples from the Yahara watershed (agricultural/urban) and the Twin Cities (urban) result in high k_C values, while samples from the

Saint Louis River tend to have lower k_C values, but all three groupings are highly varied. High variability is also observed in the seven Northern Highlands lake samples for atorvastatin and to a lesser extent sulfadiazine, which is consistent with the widely variable DOM composition in these lakes.[21,37] Similarly, a wide range of k_C values are observed for all compounds in the wastewater samples (**Figure S3**). The variability in carbon-normalized rate constants demonstrates that factors other than [DOC] play important roles in the degradation of all four contaminants.

The observation that carbamazepine, benzotriazole, sulfadiazine, and atorvastatin undergo indirect photodegradation is generally consistent with prior work using smaller numbers of DOM samples. The presence of DOM is consistently reported to increase the photodegradation rates of carbamazepine[8,11,12,24] and atorvastatin.[8,24,70] Similarly, most studies indicate that DOM increases the photodegradation rate of benzotriazole[71,72] and sulfadiazine.[9,73,74] Additionally, decreases in k_{obs} in the presence of DOM have been observed for benzotriazole[75] and sulfadiazine[9,76] in certain cases, matching the observations found here.

Identification of key PPRI through quenching experiments. Identifying the PPRI involved in indirect photodegradation is important for ultimately making predictions about contaminant photodegradation rates in different waters. The most common approach to identify the contribution of individual PPRIs is to irradiate target compounds in the presence of DOM and a quencher that is specific to each PPRI of interest. If the observed rate constant decreases in the presence of the quencher (e.g., sorbate as a ^{3}DOM quencher), that is interpreted as indirect evidence that the selected PPRI is involved in the transformation of the target compound. Quencher experiments are relatively simple to conduct, do not require the development of additional analytical methods, and avoid the need to quantify PPRI steady-state concentrations. However, these experiments can also be difficult to interpret because even the "selective" quenchers interact

with other PPRI either directly or indirectly. For example, the ^{3}DOM and $^1O_2$ quenchers react with $^{\bullet}$OH, a highly non-selective oxidant, with similar bimolecular reaction rate constants (i.e., (1.3 – 5.8) x 10^9 M^{-1} s^{-1}; **Table S10**).[77–80] Similarly, quenching ^{3}DOM limits the formation of $^1O_2$ because ^{3}DOM is the direct precursor to $^1O_2$.[13] The precursors for $^{\bullet}$OH are not well understood, but ^{3}DOM may be involved in the production of $^{\bullet}$OH.[12,81] Therefore, we use a holistic approach to compare quencher experiment results using a subset of DOM samples with regression analysis with PPRI production to identify the PPRI involved in the indirect photodegradation of atorvastatin, benzotriazole, carbamazepine, and sulfadiazine.

The involvement of ^{3}DOM is first investigated using sorbate as a quencher. With the exception of atorvastatin in Trout Bog (N2), the addition of sorbate decreases the k_{obs} values for all compounds (**Figure 2**). Quenched rate constants vary widely for atorvastatin (average: 56.1 ± 23.3% of k_{obs}), carbamazepine (10.3 ± 12.7% of k_{obs}), sulfadiazine (26.5 ± 19.0% of k_{obs}), and benzotriazole (36.4 ± 31.0% of k_{obs}) in the presence of the ^{3}DOM quencher compared to unquenched samples. The decreases in k_{obs} as a result of ^{3}DOM quenching indicate that ^{3}DOM, either directly or indirectly, plays a role in the degradation of all four compounds. The potential involvement of ^{3}DOM agrees with past studies suggesting a similar mechanism for three of the compounds,[8,9,11,12,24,70] with the exception of benzotriazole.

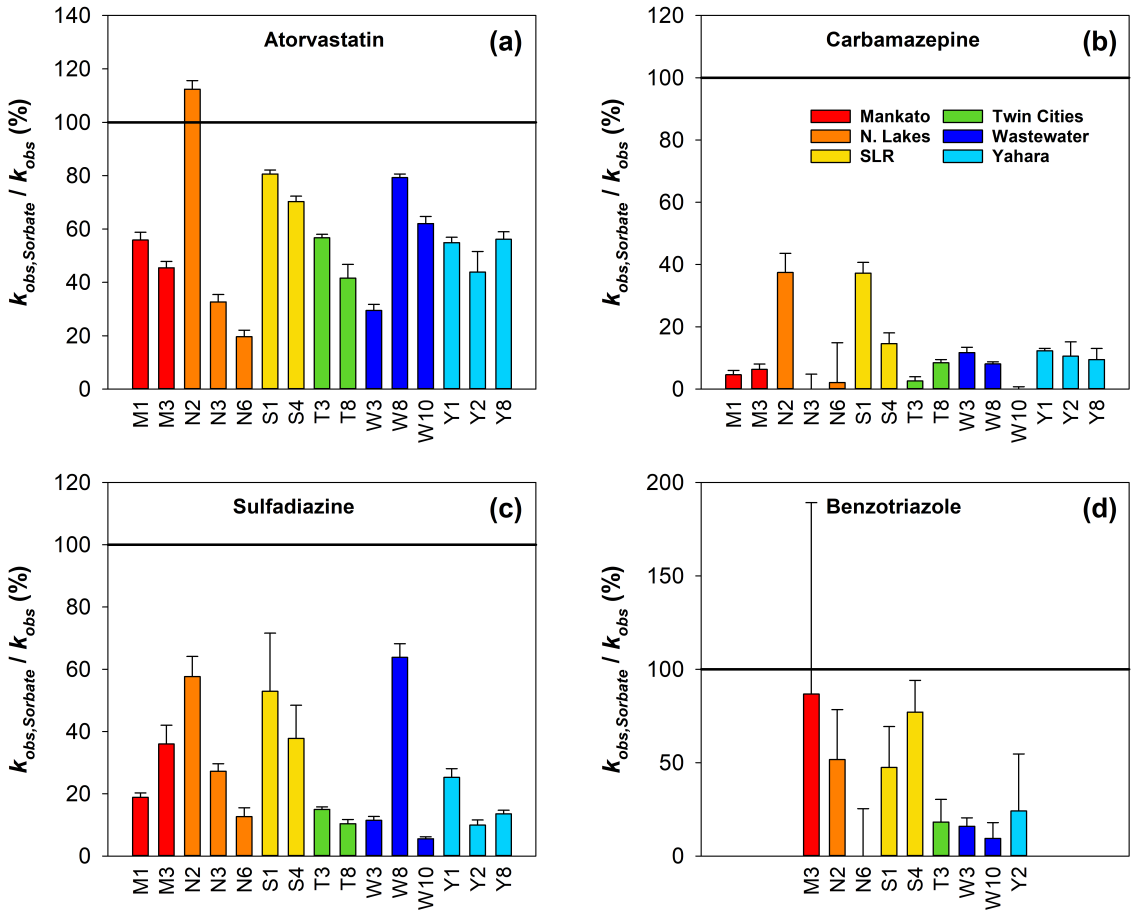

Figure 2. The relative change in observed rate constants in the presence of sorbate (i.e., the ^{3}DOM quencher) compared to unquenched samples for (a) atorvastatin, (b) carbamazepine, (c) sulfadiazine, and (d) benzotriazole. All rate constants are expressed as a percent of unquenched rate constants. The solid horizontal line represents the unquenched rate (i.e., 100%). Error bars correspond to the standard deviation of triplicate measurements.

Quenching of $^1O_2$ with histidine or DABCO also results in decreases in k_{obs} for all four compounds, indicating that $^1O_2$ also participates in the indirect photodegradation. The observed rate constant of atorvastatin decreases in all but three samples in the presence of histidine, with an average loss of 78.8 ± 22.0% compared to k_{obs} in the absence of the quencher (**Figure 3**). Compared to atorvastatin, much larger decreases due to $^1O_2$ quenching are observed for carbamazepine (31.1 ± 31.9% of k_{obs}) and sulfadiazine (19.8 ± 19.9% of k_{obs}). The impact of DABCO on benzotriazole photodegradation is highly variable (45.6 ± 31.8% of k_{obs}). The $^1O_2$ quenching data indicates that

this PPRI is very important for carbamazepine and sulfadiazine, moderately important for benzotriazole, and less important for atorvastatin. Previous studies highlight the potential importance of $^1O_2$ for atorvastatin, sulfadiazine, and carbamazepine, but argue that it is unimportant for benzotriazole,[72] which is contradictory to the quencher experiment data in this study.

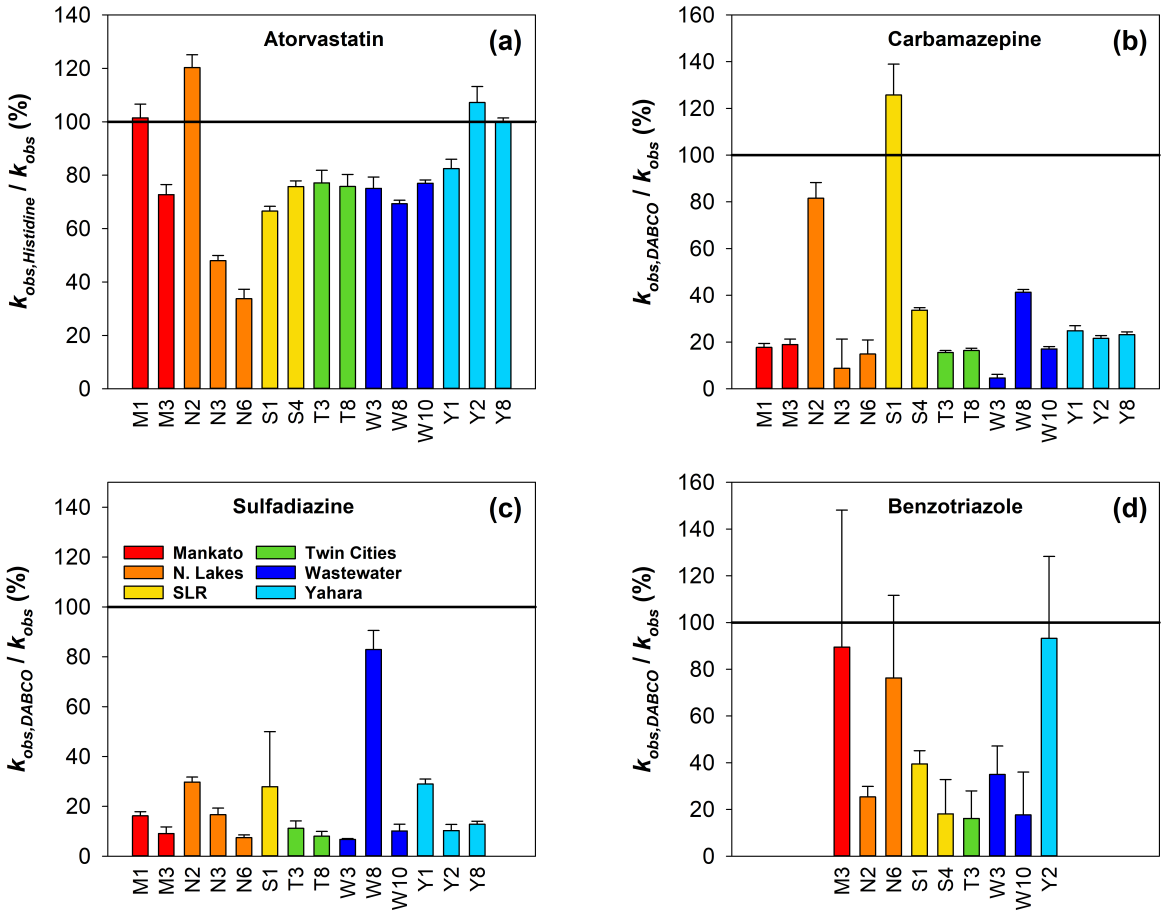

Figure 3. The relative change in observed rate constants in the presence of a $^1O_2$ quencher compared to unquenched samples for (a) atorvastatin, (b) carbamazepine, (c) sulfadiazine, and (d) benzotriazole. All rate constants are expressed as a percent of unquenched rate constants. The solid horizontal line represents the unquenched rate (i.e., 100%). Error bars correspond to the standard deviation of triplicate measurements.

While the quenching data indicate that both ^{3}DOM and $^1O_2$ are potentially involved in the indirect photodegradation of the four target compounds, it is not possible to use this data to quantify the role of each PPRI using these experiments as done previously for other compounds

(e.g., pesticides).[1,3] In many cases, the ^{3}DOM and $^1O_2$ quenchers each decrease k_{obs} to similar extents. For example, the sorbate data suggests ^{3}DOM is responsible for 89.7% of carbamazepine photodegradation on average, while the DABCO data suggests $^1O_2$ is responsible for 68.9% of loss on average (**Figures 2** and **3**). In other words, this data suggests ^{3}DOM and $^1O_2$ are responsible for >150% of indirect photolysis, which is not physically possible. Therefore, the quencher experiments either overestimate or double count the importance of each PPRI.

Additional experiments are conducted in nitrogen-sparged solutions to validate the importance of ^{3}DOM in selected samples. Because ^{3}DOM is predominantly quenched by O_2, this PPRI has a longer lifetime in the absence of oxygen.[13] Therefore, increased reaction rates provide evidence of the importance of ^{3}DOM, while decreased reaction rates provide evidence of the importance of reactive oxygen species, such as $^1O_2$. Carbamazepine photodegradation rate constants increase dramatically in all nitrogen-sparged solutions, with rate constants >3,500% of k_{obs} in air-saturated solutions (average: 9,050 ± 8,060%; **Figure S4b**). The rate constants of sulfadiazine increase in four samples and decrease in one sample (average: 255 ± 147%; **Figure S4c**). Similarly, the benzotriazole rate constant increases in seven samples and decreases in one sample (average: 176 ± 124%; **Figure S4d**). Atorvastatin photodegradation rates increase in two samples and decrease in two samples (average: 158 ± 198%; **Figure S4a**). These changes in rate constants under nitrogen sparging demonstrate that ^{3}DOM plays a major role in carbamazepine degradation, while contributing to the degradation of atorvastatin, benzotriazole, and sulfadiazine in some cases. The decreases in the degradation of these three compounds under some conditions further indicates that other PPRI (e.g., $^1O_2$ or $^{\bullet}OH$) are important. Previous studies on carbamazepine[24] and atorvastatin[70] demonstrate that oxygen removal leads to increased rate constants. This variability in the importance of ^{3}DOM is likely due to the complex nature of ^{3}DOM,

which exists at varying energy states and oxidation potentials. The sorbate quencher used in this study primarily quenches high energy ^{3}DOM,[82] but different populations of ^{3}DOM could impact its perceived importance from quenching experiments.

Quenching experiments with isopropanol clearly show the role of $^{\bullet}$OH in the indirect photodegradation of only one of the four compounds. The $^{\bullet}$OH quencher results in large decreases in the observed benzotriazole photodegradation rate constant in all tested waters (average: 34.8 ± 24.0% of k_{obs}; **Figure 4d**), which demonstrates that this PPRI is instrumental in the degradation of benzotriazole and is in agreement with a previous study.[72] In contrast, minimal changes are observed for atorvastatin (98.2 ± 21.8%) and carbamazepine (96.0 ± 18.9%), with small decreases compared to k_{obs} observed in a small number of oligotrophic lake or wastewater-impacted samples (**Figure 4**). Previous studies are contradictory in terms of the role of $^{\bullet}$OH in atorvastatin and carbamazepine degradation. Some studies indicate $^{\bullet}$OH is important in some waters[8,11,12,24] and others suggest that it is unimportant compared to $^1O_2$ and ^{3}DOM.[70,83] Finally, small changes are also observed for sulfadiazine (113.2 ± 24.3%), with modest increases in k_{obs} in several water samples.

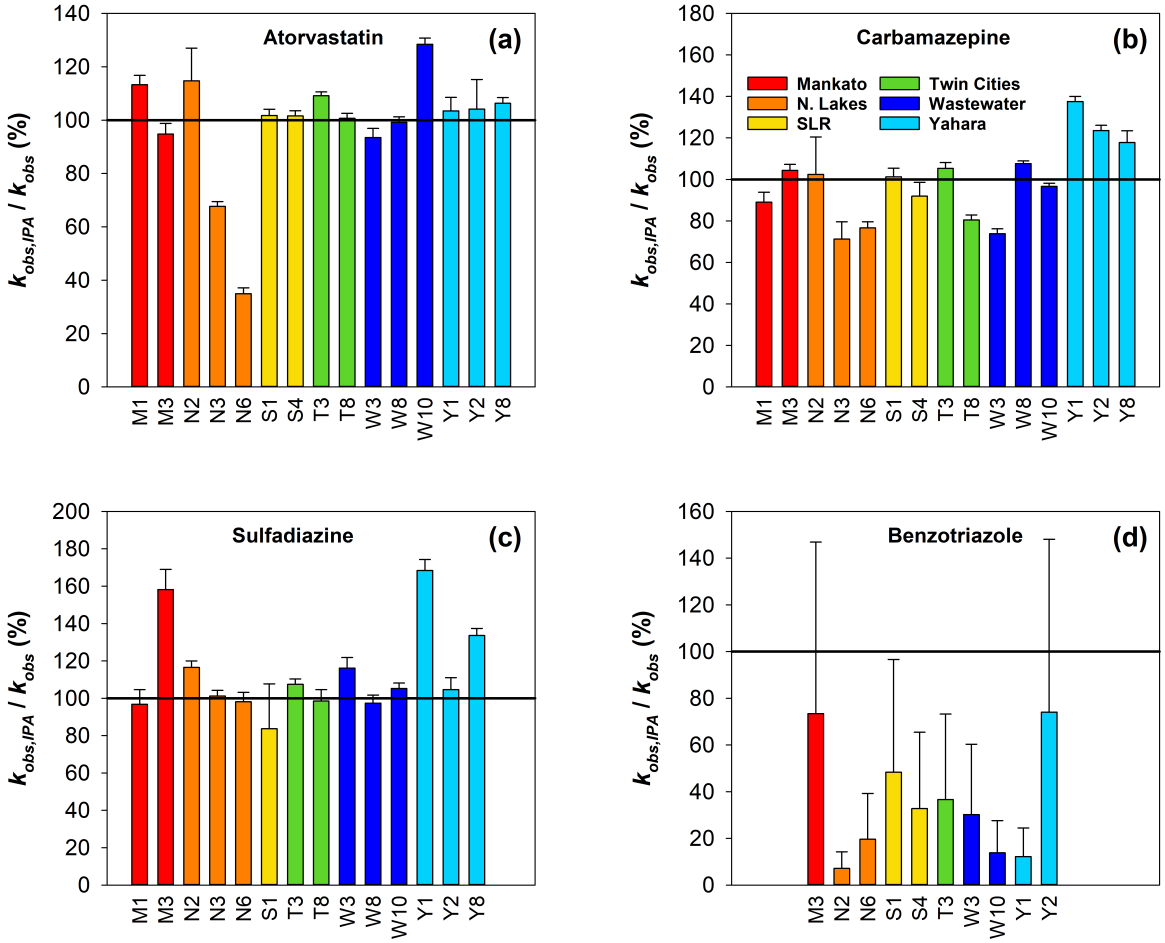

Figure 4. The relative change in observed rate constants in the presence of isopropanol (i.e., the $^{\bullet}$OH quencher) compared to unquenched samples for (a) atorvastatin, (b) carbamazepine, (c) sulfadiazine, and (d) benzotriazole. All rate constants are expressed as a percent of unquenched rate constants. The solid horizontal line represents the unquenched rate (i.e., 100%). Error bars correspond to the standard deviation of triplicate measurements.

The quencher experiments yield mixed results concerning the importance of each studied PPRI (**Table S11**). In the case of benzotriazole, the isopropanol experiments strongly indicate that $^{\bullet}$OH is a major contributor to the indirect photodegradation of this compound. It is therefore likely that some of the inhibition observed in the presence of the ^{3}DOM and $^{1}O_2$ quenchers is attributable to scavenging of $^{\bullet}$OH given the similarity in rate constants between all studied quenchers and $^{\bullet}$OH (**Table S10**). However, the nitrogen-sparging data indicates that ^{3}DOM can play a minor role in benzotriazole degradation in some cases. Both ^{3}DOM and $^{1}O_2$ appear to play a role in the

degradation of carbamazepine, atorvastatin, and sulfadiazine, with ^{3}DOM being most important for carbamazepine based on nitrogen-sparging data (**Figures 2, 3,** and **S4**). Furthermore, it is likely that some of the "^{3}DOM" quenching when sorbate is used is attributable to decreased $^1O_2$ production. While quenching experiments are a simple way to assess the potential for PPRI reactivity with target compounds, this data must be interpreted carefully because the quenchers are not truly selective for individual PPRI and because their presence can alter the formation of other PPRI.

Relationships between DOM composition, PPRI formation, and contaminant degradation. As an alternate approach to identifying the PPRI responsible for the indirect photodegradation of the four target compounds, we conduct simple linear regressions analysis between indirect photodegradation rate constants and measures of DOM composition and photoreactivity. We use two different data sets for this analysis. First, we relate indirect rate constants ($k_{indirect}$) with measurements of dissolved organic carbon concentration ([DOC]) and steady-state concentrations of each PPRI. Second, we relate carbon-normalized indirect rate constants (k_C) with carbon-normalized parameters related to DOM composition (i.e., $SUVA_{254}$, E_2:E_3, HIX, FI, H:C_w, O:C_w, and DBE_w) and quantum yields or quantum yield coefficients. All data is transformed to achieve a normal distribution if necessary (**Section S8**). Compared to quencher experiments, the quantification of individual PPRI is more selective[16] and it is therefore possible to relate the production of each PPRI with trends observed in $k_{indirect}$. This approach also facilitates the analysis of the roles of both DOM concentration and composition through correlations with [DOC] and carbon-normalized DOM composition parameters. However, this approach is more labor-intensive because it requires the quantification of PPRI individually. Furthermore, ^{3}DOM and $^1O_2$ are often highly correlated,[13,37] so it can be challenging to distinguish

between the two PPRI. For this reason, we did not conduct multiple linear regression analysis because of collinearity in key parameters of interest, such as quantum yields.

Significant positive correlations are observed between $k_{indirect}$ and measured PPRI steady-state concentrations for each of the four compounds, suggesting that the formation of individual PPRI contribute to the degradation of each contaminant. The indirect rate constants of atorvastatin and carbamazepine are positively correlated with $[^1O_2]_{ss}$ with p-values of 3.4 x 10^{-12} and 4.6 x 10^{-6} respectively (**Figures 5a** and **5b**). Indirect rate constants of atorvastatin, carbamazepine, and sulfadiazine are positively correlated with $[^3DOM]_{ss}$ (p-values = 1.1 x 10^{-3}, 2.8 x 10^{-5}, and 7.1 x 10^{-4}, respectively; **Figures S5b**, **S6b**, and **5c**), while the indirect rate of benzotriazole is negatively correlated with $[^3DOM]_{ss}$ (p-value = 4.7 x 10^{-2}; **Figure S7b**). Finally, $k_{indirect}$ of benzotriazole (p-value = 3.1 x 10^{-4}; **Figure 5d**), carbamazepine (p-value = 2.2 x 10^{-4}; **Figure S6a**), and atorvastatin (p-value = 1.1 x 10^{-2}; **Figure S5c**) are positively correlated with $[^{\bullet}OH]_{ss}$. Based on the strength of the correlations, $[^1O_2]_{ss}$ is most important for atorvastatin and carbamazepine, $[^3DOM]_{ss}$ is most important for sulfadiazine, and $[^{\bullet}OH]_{ss}$ is most important for benzotriazole.

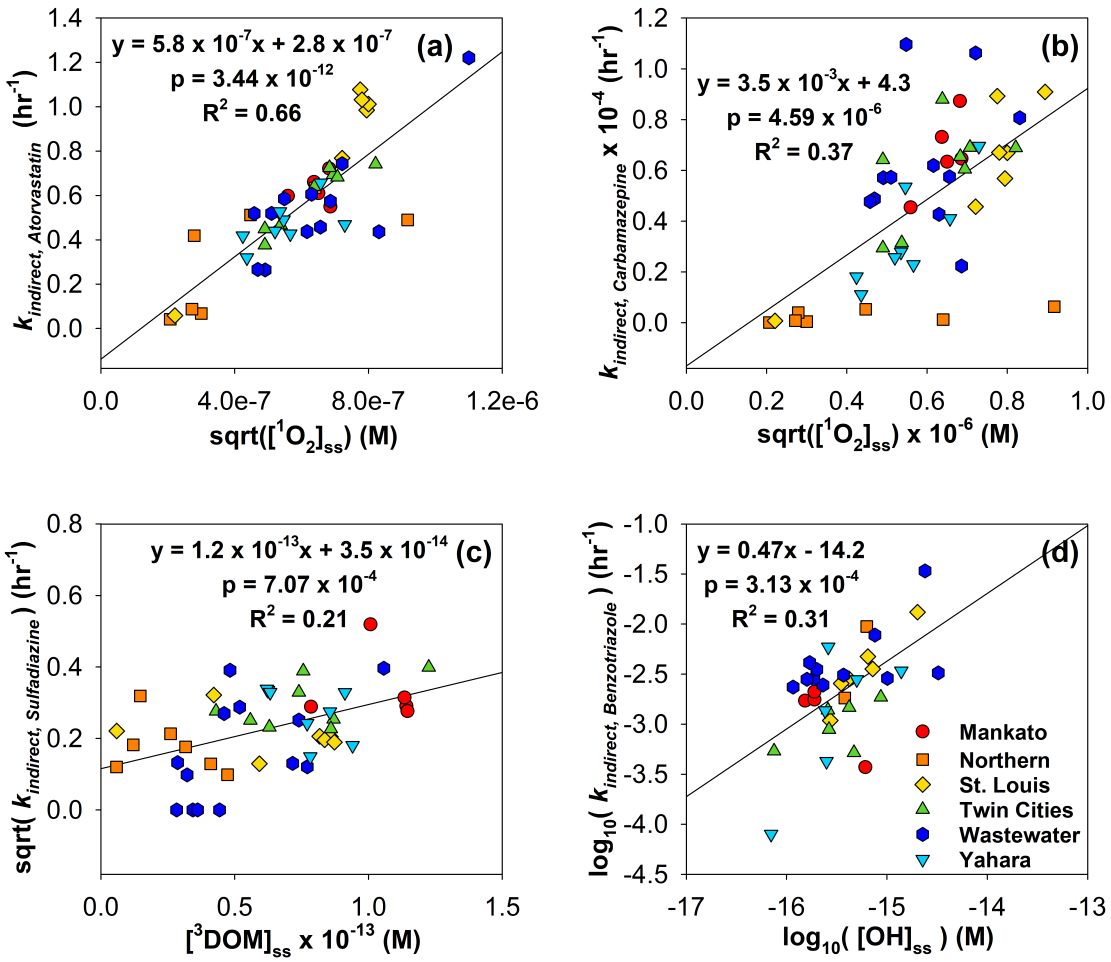

Figure 5. Linear regression analysis for (a) $[^1O_2]_{ss}$ and $k_{indirect,atorvastatin}$, (b) $[^1O_2]_{ss}$ and $k_{indirect,carbamazepine}$, (c) $[^3DOM]_{ss}$ and $k_{indirect,sulfadiazine}$, and (d) $[^{\bullet}OH]_{ss}$ and $k_{indirect,benzotriazole}$. All correlations are statistically significant ($p < 0.05$). The strongest correlation for each compound is presented here; additional correlations with $k_{indirect}$ values are presented in **Figure S5 – S7**. Parameters were transformed as listed in axes labels to achieve a normal distribution if necessary.

Similar correlations are also observed between carbon-normalized indirect rate constants (k_C) and PPRI quantum yields and/or quantum yield coefficients. The k_C values for atorvastatin (p-value = 3.5 x 10^{-4}; **Figure 6a**, carbamazepine (p-value = 1.5 x 10^{-6}; **Figure S9c**), and sulfadiazine (p-value = 6.8 x 10^{-5}; **Figure S10c**) are positively correlated with f_{TMP}. Consistent positive trends are also observed for all four compounds with Φ_{1O2}, with carbamazepine and sulfadiazine showing the strongest relationships (p-values = 7.8 x 10^{-9} and 9.9 x 10^{-7}, respectively; **Figures 6b** and **6c**). Significant trends are observed with $\Phi_{\bullet OH}$ for benzotriazole (positive; p-value = 2.9 x 10^{-2}; **Figure**

6d) and sulfadiazine (negative; p-value = 3.1 x 10^{-2}; **Figure S10d**). These regression analyses suggest that both ^{3}DOM and $^1O_2$ are important for carbamazepine, atorvastatin, and sulfadiazine, while sulfadiazine has a weak negative correlation with $^{\bullet}$OH. Benzotriazole has only weak correlations with $^1O_2$ and $^{\bullet}$OH, which is surprising given the results of the quenching experiments and the $k_{indirect}$ regression analysis.

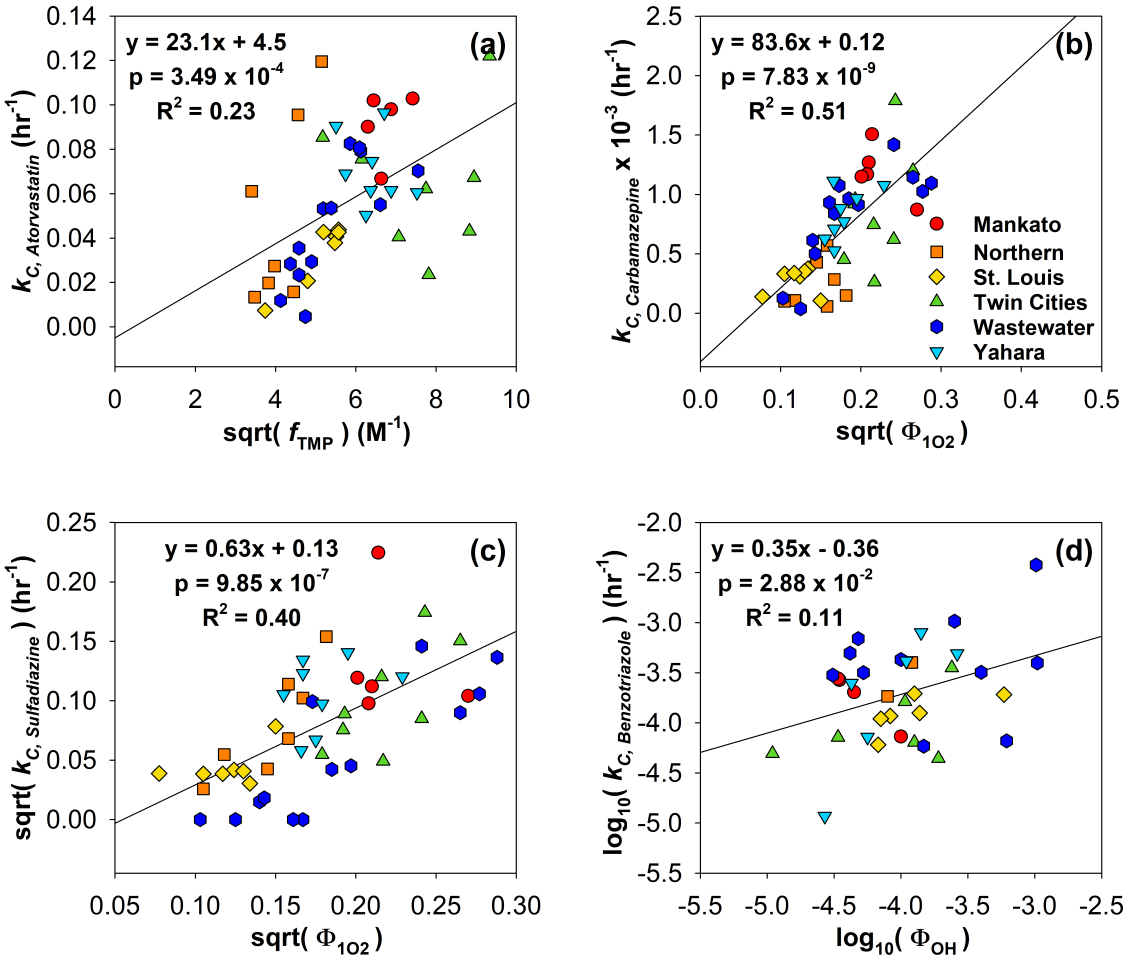

Figure 6. Linear regression analysis for (a) f_{TMP} and $k_{C,atorvastatin}$, (b) Φ_{1O2} and $k_{C,carbamazepine}$, (c) Φ_{1O2} and $k_{Csulfadiazine}$, and (d) FI and $k_{C,benzotriazole}$. All correlations are statistically significant ($p < 0.05$). The strongest correlation for each compound with PPRI quantum yields and/or quantum yield coefficients is presented here; additional correlations with k_C values with other PPRIs and with DOM composition parameters are presented in **Figures S8 – S11**. Parameters were transformed as listed in axes labels to achieve a normal distribution if necessary.

This analysis is also used to assess whether DOM concentration or composition is the key driver of indirect photodegradation. Simple linear regression analysis demonstrates that [DOC] is not the sole parameter responsible for the indirect photodegradation trends observed in the 48 samples. The indirect rate constants of atorvastatin and benzotriazole are positively correlated with [DOC] (p-values = 4.1×10^{-7} and 3.7×10^{-2}, respectively; **Figure S5a** and **S7a**), while $k_{indirect}$ for sulfadiazine and carbamazepine are not significantly correlated with [DOC].

The linear regressions between carbon-normalized rate constants and DOM composition parameters indicate that DOM composition plays a key role in indirect photodegradation. For example, both carbamazepine and benzotriazole k_C values are positively correlated with FI (**Figure S9b** and **11d**), while carbamazepine k_C values are negatively correlated with HIX (**Figure S9a**). Furthermore, sulfadiazine k_C values are positively correlated with E_2:E_3 (**Figure S10a**) and negatively correlated with EDC (**Figure S10b**). Collectively, higher carbon-normalized indirect photodegradation rates are observed in waters that have DOM that is less aromatic, lower in molecular weight, and microbial in nature. Previous studies have demonstrated that this type of DOM (e.g., in wastewater effluent or in eutrophic lakes) is more efficient at generating PPRI such as ^{3}DOM and $^1O_2$.[21,24,35,37] In contrast, carbon-normalized rate constants for atorvastatin have weak negative correlations with H:C_w (**Figure S8a**) and weak positive correlations with DBE_w (**Figure S8c**), suggesting that atorvastatin degradation is associated with more aromatic DOM.

Conclusions and Recommendations for Indirect Photolysis Studies

Using a sample set of 48 waters that range widely in DOM composition, we show that atorvastatin, carbamazepine, sulfadiazine, and benzotriazole undergo indirect photodegradation in all but 15 of 192 contaminant/DOM pairs. Thus, indirect photodegradation is likely to be more

important than direct photodegradation in the majority of surface waters and wastewater-impacted sites for these target compounds. Furthermore, this work highlights that water type and DOM composition are important factors in indirect photodegradation of contaminants.

Identification of the PPRI involved in indirect photodegradation is important for predicting the rate of this process in sunlit waters. Quencher studies designed to inhibit certain PPRI indicate that ^{3}DOM, and to a lesser extent $^1O_2$, play important roles in the degradation of all four contaminants. ^{3}DOM is more important for atorvastatin, carbamazepine, and benzotriazole, while $^1O_2$ is more important for sulfadiazine. Nitrogen sparging, which increases the lifetime of ^{3}DOM, has the greatest increase in carbamazepine rate constants. In comparison, $^{\bullet}$OH is identified as a key PPRI only for benzotriazole. However, the ^{3}DOM and $^1O_2$ quenchers also quench $^{\bullet}$OH; thus, data generated using these quenchers should be interpreted cautiously for compounds that also react with $^{\bullet}$OH. Similar to the quenching studies, linear regression analysis demonstrates that ^{3}DOM plays an important role in the degradation of all compounds but benzotriazole and $^1O_2$ plays a role in the degradation of all compounds. $^{\bullet}$OH is identified as important for benzotriazole, but also for carbamazepine and atorvastatin, which is dissimilar to the results of quenching experiments.

Overall, both quencher studies and regression analysis provide useful but imperfect information regarding the importance of individual PPRI. Linear regression analysis is able to identify trends across a large number of samples, but it does not address the variability seen in individual samples. The requirement of having a large sample set of natural waters in which to quantify steady-state concentrations and quantum yields also limits its application. In contrast, quencher studies can be performed with a small sample set, but double count or overcount the contribution of PPRIs, particularly $^1O_2$ and ^{3}DOM. While we anticipate that quencher experiments

will remain the standard approach for identifying PPRI due to their ease of use and smaller data requirement, we offer the following suggestions for improved data interpretation:

(1) For a given compound, it is important to analyze all three key PPRI (i.e., ^{3}DOM, $^1O_2$, and $^{\bullet}$OH) and not rely on a single quencher. For example, decreased observed rate constants in the presence of sorbate could be due to direct reaction of the quencher with ^{3}DOM, prevention of $^1O_2$ formation by quenching ^{3}DOM, or simply scavenging of $^{\bullet}$OH.

(2) When possible, supplemental experiments can provide more mechanistic evidence. Removal of oxygen (e.g., via nitrogen sparging) can either provide or rule out direct ^{3}DOM reactivity with the target compound. Furthermore, while only possible in studies using DOM isolates, the use of deuterated solvents (e.g., D_2O) can provide evidence of $^1O_2$.[13,84]

(3) Trends in DOM-mediated indirect photodegradation can vary widely with the type of DOM used. We used a large data set to draw general conclusions, but note that there are individual samples with different trends in several cases. Thus, caution should be used when interpretating data generated from a small number of samples or from samples with highly similar DOM composition.

Finally, conducting linear regression analysis with a large number of highly variable samples enabled us to test the roles of DOM concentration and composition in indirect photodegradation. The correlations with [DOC] were inconsistent; we observed positive trends for atorvastatin and benzotriazole and no trend for carbamazepine and sulfadiazine. In contrast, there were clear correlations between indirect rate constants for atorvastatin, carbamazepine, sulfadiazine, and benzotriazole with DOM composition parameters. We observed that DOM that

is lower in apparent molecular weight (high E_2:E_3), more electron poor (low EDC), and more microbial-like (high FI, low HIX) was strongly associated with the carbon-normalized indirect photodegradation rates for benzotriazole, carbamazepine, and sulfadiazine, with weak correlations observed for atorvastatin. Therefore, we conclude that DOM composition influences the indirect photodegradation of target compounds, as observed previously in smaller sets of samples[24] and as observed for the formation of PPRI in general.[21,28,37,51]

Acknowledgements

This work was supported by the National Science Foundation (CBET-1802388). The authors acknowledge the North Temperate Lakes-Long Term Ecological Research Network for assistance in sample collection (DEB-2025982). We acknowledge the UW-Madison Human Proteomics Program Mass Spectrometry Facility for support in obtaining mass spectrometry data, Yanlong Zhu for assistance with instrument operation, and NIH S10OD018475 for acquisition of the high-resolution mass spectrometer. We also acknowledge Noah Lottig, Josh Gad, Ben Peterson, Amber White, Matt Seib, Joseph Herrli, Ronan Winkels, Kailey Beer, and Alyssa Risch for their support in sample collection.

Electronic Supplementary Information

Additional information on materials, kinetics experiments and corresponding HPLC methods, linear regression analysis, and quenching experiments can be found in the Electronic Supplementary Information.

References

(1) Zeng, T.; Arnold, W. A. Pesticide photolysis in prairie potholes: Probing photosensitized processes. *Environ. Sci. Technol.* **2013**, *47* (13), 6735–6745.

(2) McConville, M. B.; Hubert, T. D.; Remucal, C. K. Direct photolysis rates and transformation pathways of the lampricides TFM and niclosamide in simulated sunlight. *Environ. Sci. Technol.* **2016**, *50* (18), 9998–10006.

(3) McConville, M. B.; Mezyk, S. P.; Remucal, C. K. Indirect photodegradation of the lampricides TFM and niclosamide. *Environ. Sci. Process. Impacts* **2017**, *19* (8), 1028–1039.

(4) White, A. M.; Nault, M. E.; McMahon, K. D.; Remucal, C. K. Synthesizing laboratory and field experiments to quantify dominant transformation mechanisms of 2,4-dichlorophenoxyacetic acid (2,4-D) in aquatic environments. *Environ. Sci. Technol.* **2022**, *56* (15), 10838–10848.

(5) Boreen, A. L.; Arnold, W. A.; McNeill, K. Photodegradation of pharmaceuticals in the aquatic environment: a review. *Aquat. Sci.* **2003**, *65* (4), 320–341.

(6) Remucal, C. K. The role of indirect photochemical degradation in the environmental fate of pesticides: a review. *Environ. Sci. Process. Impacts* **2014**, *16* (4), 628–653.

(7) Miller, P. L.; Chin, Y. P. Indirect photolysis promoted by natural and engineered wetland water constituents: Processes leading to alachlor degradation. *Environ. Sci. Technol.* **2005**, *39* (12), 4454–4462.

(8) Lam, M. W.; Mabury, S. A. Photodegradation of the pharmaceuticals atorvastatin, carbamazepine, levofloxacin, and sulfamethoxazole in natural waters. *Aquat. Sci.* **2005**, *67* (2), 177–188.

(9) Bahnmüller, S.; von Gunten, U.; Canonica, S. Sunlight-induced transformation of sulfadiazine and sulfamethoxazole in surface waters and wastewater effluents. *Water Res.* **2014**, *57*, 183–192.

(10) Torrents, A.; Anderson, B. G.; Bilboulian, S.; Johnson, W. E.; Hapeman, C. J. Atrazine photolysis: mechanistic investigations of direct and nitrate-mediated hydroxy radical processes and the influence of dissolved organic carbon from the Chesapeake Bay. *Environ. Sci. Technol.* **1997**, *31* (5), 1476–1482.

(11) Carlos, L.; Mártire, D. O.; Gonzalez, M. C.; Gomis, J.; Bernabeu, A.; Amat, A. M.; Arques, A. Photochemical fate of a mixture of emerging pollutants in the presence of humic substances. *Water Res.* **2012**, *46* (15), 4732–4740.

(12) Dong, M. M.; Trenholm, R.; Rosario-Ortiz, F. L. Photochemical degradation of atenolol, carbamazepine, meprobamate, phenytoin and primidone in wastewater effluents. *J. Hazard. Mater.* **2015**, *282*, 216–223.

(13) McNeill, K.; Canonica, S. Triplet state dissolved organic matter in aquatic photochemistry: reaction mechanisms, substrate scope, and photophysical properties. *Environ. Sci. Process. Impacts* **2016**, *18* (11), 1381–1399.

(14) Goldstone, J. V.; Pullin, M. J.; Bertilsson, S.; Voelker, B. M. Reactions of hydroxyl radical with humic substances: Bleaching, mineralization, and production of bioavailable carbon substrates. *Environ. Sci. Technol.* **2002**, *36* (3), 364–372.

(15) Cory, R. M.; McNeill, K.; Cotner, J. P.; Amado, A.; Purcell, J. M.; Marshall, A. G. Singlet oxygen in the coupled photochemical and biochemical oxidation of dissolved organic matter. *Environ. Sci. Technol.* **2010**, *44* (10), 3683–3689.

(16) Rosario-Ortiz, F. L.; Canonica, S. Probe compounds to assess the photochemical activity of dissolved organic matter. *Environ. Sci. Technol.* **2016**, *50* (23), 12532–12547

(17) Vione, D.; Minella, M.; Maurino, V.; Minero, C. Indirect photochemistry in sunlit surface waters: Photoinduced production of reactive transient species. *Chem. Eur. J.* **2014**, *20* (34), 10590–10606.

(18) Khetan, S. K.; Collins, T. J. Human pharmaceuticals in the aquatic environment: a challenge to green chemistry. *Chem. Rev.* **2007**, *107* (6), 2319–2364.

(19) Stephens, B. M.; Minor, E. C. DOM characteristics along the continuum from river to receiving basin: a comparison of freshwater and saline transects. *Aquat. Sci.* **2010**, *72* (4), 403–417.

(20) Peterson, B. M.; McNally, A. M.; Cory, R. M.; Thoemke, J. D.; Cotner, J. B.; McNeill, K. Spatial and temporal distribution of singlet oxygen in Lake Superior. *Environ. Sci. Technol.* **2012**, *46* (13), 7222–7229.

(21) Maizel, A. C.; Li, J.; Remucal, C. K. Relationships between dissolved organic matter composition and photochemistry in lakes of diverse trophic status. *Environ. Sci. Technol.* **2017**, *51* (17), 9624–9632.

(22) Berg, S. M.; Mooney, R. J.; McConville, M. B.; McIntyre, P. B.; Remucal, C. K. Seasonal and spatial variability of dissolved carbon concentration and composition in Lake Michigan tributaries. *J. Geophys. Res. Biogeosci.* **2021**, *126* (10), e2021JG006449.

(23) Milstead, R. P.; Remucal, C. K. Molecular-level insights into the formation of traditional and novel halogenated disinfection byproducts. *ACS ES&T Water* **2021**, *1* (8), 1966–1974.

(24) Berg, S. M.; Whiting, Q. T.; Herrli, J. A.; Winkels, R.; Wammer, K. H.; Remucal, C. K. The role of dissolved organic matter composition in determining photochemical reactivity at the molecular level. *Environ. Sci. Technol.* **2019**, *53* (20), 11725–11734.

(25) Milstead, R. P.; Horvath, E. R.; Remucal, C. K. Dissolved organic matter composition determines its susceptibility to complete and partial photooxidation within lakes. *Environ. Sci. Technol.* **2023**, *57* (32), 11876–11885.

(26) Remucal, C. K.; Cory, R. M.; Sander, M.; McNeill, K. Low molecular weight components in an aquatic humic substance as characterized by membrane dialysis and Orbitrap mass spectrometry. *Environ. Sci. Technol.* **2012**, *46* (17), 9350–9359.

(27) Weishaar, J. L.; Aiken, G. R.; Bergamaschi, B. A.; Fram, M. S.; Fujii, R.; Mopper, K. Evaluation of specific ultraviolet absorbance as an indicator of the chemical composition and reactivity of dissolved organic carbon. *Environ. Sci. Technol.* **2003**, *37* (20), 4702–4708.

(28) McCabe, A. J.; Arnold, W. A. Reactivity of triplet excited states of dissolved natural organic matter in stormflow from mixed-use watersheds. *Environ. Sci. Technol.* **2017**, *51* (17), 9718–9728.

(29) Frimmel, F. H.; Bauer, H.; Putzien, J.; Murasecco, P.; Braun, A. M. Laser flash photolysis of dissolved aquatic humic material and the sensitized production of singlet oxygen. *Environ. Sci. Technol.* **1987**, *21* (6), 541–545.

(30) Cavani, L.; Halladja, S.; ter Halle, A.; Guyot, G.; Corrado, G.; Ciavatta, C.; Boulkamk, A.; Richard, C. Relationship between photosensitizing and emission properties of peat humic acid fractions obtained by tangential ultrafiltration. *Environ. Sci. Technol.* **2009**, *43* (12), 4348-4354.

(31) Chin, Y. P.; Aiken, G.; O'Loughlin, E. Molecular weight, polydispersity, and spectroscopic properties of aquatic humic substances. *Environ. Sci. Technol.* **1994**, *28* (11), 1853–1858.

(32) Sandvik, S. L. H.; Bilski, P.; Pakulski, J. D.; Chignell, C. F.; Coffin, R. B. Photogeneration of singlet oxygen and free radicals in dissolved organic matter isolated from the Mississippi and Atchafalaya River plumes. *Mar. Chem.* **2000**, *69* (1), 139–152.

(33) Aguer, J. P.; Trubetskaya, O.; Trubetskoj, O.; Richard, C. Photoinductive properties of soil humic acids and their fractions obtained by tandem size exclusion chromatography-polyacrylamide gel electrophoresis. *Chemosphere* **2001**, *44* (2), 205–209.

(34) Haag, W. R.; Hoigne, Juerg. Singlet oxygen in surface waters. 3. Photochemical formation and steady-state concentrations in various types of waters. *Environ. Sci. Technol.* **1986**, *20* (4), 341–348.

(35) Mostafa, S.; Rosario-Ortiz, F. L. Singlet oxygen formation from wastewater organic matter. *Environ. Sci. Technol.* **2013**, *47* (15), 8179–8186.

(36) McKay, G.; Huang, W.; Romera-Castillo, C.; Crouch, J. E.; Rosario-Ortiz, F. L.; Jaffé, R. Predicting reactive intermediate quantum yields from dissolved organic matter photolysis using optical properties and antioxidant capacity. *Environ. Sci. Technol.* **2017**, *51* (10), 5404–5413.

(37) Berg, S. M.; Wammer, K. H.; Remucal, C. K. Dissolved organic matter photoreactivity is determined by its optical properties, redox activity, and molecular composition. *Environ. Sci. Technol.* **2023**, *57* (16), 6703–6711.

(38) Baldwin, A. K.; Corsi, S. R.; De Cicco, L. A.; Lenaker, P. L.; Lutz, M. A.; Sullivan, D. J.; Richards, K. D. Organic contaminants in Great Lakes tributaries: Prevalence and potential aquatic toxicity. *Sci. Total Environ.* **2016**, *554–555*, 42–52.

(39) Gruden, C. L.; Dow, S. M.; Hernandez, M. T. Fate and toxicity of aircraft deicing fluid additives through anaerobic digestion. *Water Environ. Res.* **2001**, *73* (1), 72–79.

(40) Weidauer, C.; Davis, C.; Raeke, J.; Seiwert, B.; Reemtsma, T. Sunlight photolysis of benzotriazoles – Identification of transformation products and pathways. *Chemosphere* **2016**, *154*, 416–424.

(41) Alotaibi, M. D.; McKinley, A. J.; Patterson, B. M.; Reeder, A. Y. Benzotriazoles in the aquatic environment: A review of their occurrence, toxicity, degradation and analysis. *Water. Air. Soil Pollut.* **2015**, *226* (7), 226.

(42) Shi, Z. Q.; Liu, Y. S.; Xiong, Q.; Cai, W. W.; Ying, G. G. Occurrence, toxicity and transformation of six typical benzotriazoles in the environment: A review. *Sci. Total Environ.* **2019**, *661*, 407–421.

(43) Helms, J. R.; Stubbins, A.; Ritchie, J. D.; Minor, E. C.; Kieber, D. J.; Mopper, K. Absorption spectral slopes and slope ratios as indicators of molecular weight, source, and photobleaching of chromophoric dissolved organic matter. *Limnol. Oceanogr.* **2008**, *53* (3), 955–969.

(44) Peuravuori, J.; Pihlaja, K. Molecular size distribution and spectroscopic properties of aquatic humic substances. *Anal. Chim. Acta* **1997**, *337* (2), 133–149.

(45) McKnight, D. M.; Boyer, E. W.; Westerhoff, P. K.; Doran, P. T.; Kulbe, T.; Andersen, D. T. Spectrofluorometric characterization of dissolved organic matter for indication of precursor organic material and aromaticity. *Limnol. Oceanogr.* **2001**, *46* (1), 38–48.

(46) Ohno, T. Fluorescence inner-filtering correction for determining the humification index of dissolved organic matter. *Environ. Sci. Technol.* **2002**, *36* (4), 742–746.

(47) Walpen, N.; Houska, J.; Salhi, E.; Sander, M.; von Gunten, U. Quantification of the electron donating capacity and UV absorbance of dissolved organic matter during

ozonation of secondary wastewater effluent by an assay and an automated analyzer. *Water Res.* **2020**, *185*, 116235.

(48) Dittmar, T.; Koch, B.; Hertkorn, N.; Kattner, G. A simple and efficient method for the solid-phase extraction of dissolved organic matter (SPE-DOM) from seawater. *Limnol. Oceanogr. Methods* **2008**, *6* (6), 230–235.

(49) Koch, B. P.; Dittmar, T.; Witt, M.; Kattner, G. Fundamentals of molecular formula assignment to ultrahigh resolution mass data of natural organic matter. *Anal. Chem.* **2007**, *79* (4), 1758–1763.

(50) Bulman, D. M.; Mezyk, S. P.; Remucal, C. K. The impact of pH and irradiation wavelength on the production of reactive oxidants during chlorine photolysis. *Environ. Sci. Technol.* **2019**, *53* (8), 4450–4459.

(51) McCabe, A. J.; Arnold, W. A. Seasonal and spatial variabilities in the water chemistry of prairie pothole wetlands influence the photoproduction of reactive intermediates. *Chemosphere* **2016**, *155*, 640–647.

(52) Page, S. E.; Arnold, W. A.; McNeill, K. Terephthalate as a probe for photochemically generated hydroxyl radical. *J. Environ. Monit.* **2010**, *12* (9), 1658–1665.

(53) Appiani, E.; Ossola, R.; E. Latch, D.; R. Erickson, P.; McNeill, K. Aqueous singlet oxygen reaction kinetics of furfuryl alcohol: Effect of temperature, pH, and salt content. *Environ. Sci. Process. Impacts* **2017**, *19* (4), 507–516.

(54) Page, S. E.; Arnold, W. A.; McNeill, K. Assessing the contribution of free hydroxyl radical in organic matter-sensitized photohydroxylation reactions. *Environ. Sci. Technol.* **2011**, *45* (7), 2818–2825.

(55) Maizel, A. C.; Remucal, C. K. The effect of probe choice and solution conditions on the apparent photoreactivity of dissolved organic matter. *Environ. Sci. Process. Impacts* **2017**, *19* (8), 1040–1050.

(56) Canonica, S.; Hellrung, B.; Wirz, J. Oxidation of phenols by triplet aromatic ketones in aqueous solution. *J. Phys. Chem. A* **2000**, *104* (6), 1226–1232.

(57) Laszakovits, J. R.; Berg, S. M.; Anderson, B. G.; O'Brien, J. E.; Wammer, K. H.; Sharpless, C. M. *p*-Nitroanisole/pyridine and *p*-nitroacetophenone/pyridine actinometers revisited: quantum yield in comparison to ferrioxalate. *Environ. Sci. Technol. Lett.* **2017**, *4* (1), 11–14.

(58) Schroer, H. W.; Londono, E.; Li, X.; Lehmler, H.-J.; Arnold, W.; Just, C. L. Photolysis of 3-nitro-1,2,4-triazol-5-one: Mechanisms and products. *ACS ES&T Water* **2023**, *3* (3), 783–792.

(59) Zhou, Z.; Chen, B.; Qu, X.; Fu, H.; Zhu, D. Dissolved black carbon as an efficient sensitizer in the photochemical transformation of 17β-estradiol in aqueous solution. *Environ. Sci. Technol.* **2018**, *52* (18), 10391–10399.

(60) Grebel, J. E.; Pignatello, J. J.; Mitch, W. A. Impact of halide ions on natural organic matter-sensitized photolysis of 17β-estradiol in saline waters. *Environ. Sci. Technol.* **2012**, *46* (13), 7128–7134.

(61) Boreen, A. L.; Arnold, W. A.; McNeill, K. Photochemical fate of sulfa drugs in the aquatic environment: Sulfa drugs containing five-membered heterocyclic groups. *Environ. Sci. Technol.* **2004**, *38* (14), 3933–3940.

(62) Maizel, A. C.; Remucal, C. K. Molecular composition and photochemical reactivity of size-fractionated dissolved organic matter. *Environ. Sci. Technol.* **2017**, *51* (4), 2113–2123.

(63) Walpen, N.; Getzinger, G. J.; Schroth, M. H.; Sander, M. Electron-donating phenolic and electron-accepting quinone moieties in peat dissolved organic matter: Quantities and redox transformations in the context of peat biogeochemistry. *Environ. Sci. Technol.* **2018**, *52* (9), 5236–5245.

(64) Aeschbacher, M.; Graf, C.; Schwarzenbach, R. P.; Sander, M. Antioxidant properties of humic substances. *Environ. Sci. Technol.* **2012**, *46* (9), 4916–4925.

(65) Berg, S. M.; Peterson, B. D.; McMahon, K. D.; Remucal, C. K. Spatial and temporal variability of dissolved organic matter molecular composition in a stratified eutrophic lake. *J. Geophys. Res. Biogeosci* **2022**, *127* (1), e2021JG006550.

(66) Jane, S. F.; Winslow, L. A.; Remucal, C. K.; Rose, K. C. Long-term trends and synchrony in dissolved organic matter characteristics in Wisconsin, USA, lakes: Quality, not quantity, is highly sensitive to climate. *J. Geophys. Res. Biogeosci* **2017**, *122* (3), 546–561.

(67) White, A. M.; Van Frost, S. R.; Jauquet, J. M.; Magness, A. M.; McMahon, K. D.; Remucal, C. K. Quantifying the role of simultaneous transformation pathways in the fate of the novel aquatic herbicide florpyrauxifen-benzyl. *Environ. Sci. Technol.* **2023**, DOI: 10.1021/acs.est.3c03343.

(68) Hixson, J. L.; Ward, A. S.; McConville, M. B.; Remucal, C. K. Release timing and duration control the fate of photolytic compounds in stream-hyporheic systems. *Water Resour. Res.* **2022**, *58* (11), e2022WR032567.

(69) McConville, M. B.; Cohen, N. M.; Nowicki, S. M.; Lantz, S. R.; Hixson, J. L.; Ward, A. S.; Remucal, C. K. A field analysis of lampricide photodegradation in Great Lakes tributaries. *Environ. Sci. Process. Impacts* **2017**, *19* (7), 891–900.

(70) Razavi, B.; Ben Abdelmelek, S.; Song, W.; O'Shea, K. E.; Cooper, W. J. Photochemical fate of atorvastatin (Lipitor) in simulated natural waters. *Water Res.* **2011**, *45* (2), 625–631.

(71) Chung, K. H.-Y.; Lin, Y.-C.; Lin, A. Y.-C. The persistence and photostabilizing characteristics of benzotriazole and 5-methyl-1H-benzotriazole reduce the photochemical behavior of common photosensitizers and organic compounds in aqueous environments. *Environ. Sci. Pollut. Res.* **2018**, *25* (6), 5911–5920.

(72) Janssen, E. M. L.; Marron, E.; McNeill, K. Aquatic photochemical kinetics of benzotriazole and structurally related compounds. *Environ. Sci. Process. Impacts* **2015**, *17* (5), 939–946.

(73) Boreen, A. L.; Arnold, W. A.; McNeill, K. Triplet-sensitized photodegradation of sulfa drugs containing six-membered heterocyclic groups: identification of an SO_2 extrusion photoproduct. *Environ. Sci. Technol.* **2005**, *39* (10), 3630–3638.

(74) Sukul, P.; Lamshöft, M.; Zühlke, S.; Spiteller, M. Photolysis of ^{14}C-sulfadiazine in water and manure. *Chemosphere* **2008**, *71* (4), 717–725.

(75) Liu, Y. S.; Ying, G. G.; Shareef, A.; Kookana, R. S.; Liu, Y. S.; Ying, G. G.; Shareef, A.; Kookana, R. S. Photolysis of benzotriazole and formation of its polymerised photoproducts in aqueous solutions under UV irradiation. *Environ. Chem.* **2011**, *8* (2), 174–181.

(76) Biošić, M.; Mitrevski, M.; Babić, S. Environmental behavior of sulfadiazine, sulfamethazine, and their metabolites. *Environ. Sci. Pollut. Res.* **2017**, *24* (10), 9802–9812.

(77) Buxton, G. V.; Greenstock, C. L.; Helman, W. P.; Ross, A. B. Critical review of rate constants for reactions of hydrated electrons, hydrogen atoms and hydroxyl radicals ($^{\bullet}OH/^{\bullet}O^{-}$) in aqueous solution. *J. Phys. Chem. Ref. Data* **1988**, *17* (2), 513–886.

(78) Aruoma, O. I.; Laughton, M. J.; Halliwell, B. Carnosine, homocarnosine and anserine: Could they act as antioxidants in vivo? *Biochem. J.* **1989**, *264* (3), 863–869.

(79) Anderson, R. F.; Patel, K. B. The effect of 1,4-diazabicyclo[2.2.2]octane on the radiosensitivity of bacteria. *Photochem. Photobiol.* **1978**, *28* (4–5), 881–885.

(80) Motohashi, N.; Saito, Y. Competitive measurement of rate constants for hydroxyl radical reactions using radiolytic hydroxylation of benzoate. *Chem. Pharm. Bull.* **1993**, *41* (10), 1842–1845.

(81) McKay, G.; Rosario-Ortiz, F. L. Temperature dependence of the photochemical formation of hydroxyl radical from dissolved organic matter. *Environ. Sci. Technol.* **2015**, *49* (7), 4147–4154.

(82) Moor, K. J.; Schmitt, M.; Erickson, P. R.; McNeill, K. Sorbic acid as a triplet probe: triplet energy and reactivity with triplet-state dissolved organic matter via $^1O_2$ phosphorescence. *Environ. Sci. Technol.* **2019**, *53* (14), 8078–8086.

(83) Cermola, F.; DellaGreca, M.; Iesce, M. R.; Montanaro, S.; Previtera, L.; Temussi, F. Photochemical behavior of the drug atorvastatin in water. *Tetrahedron* **2006**, *62* (31), 7390–7395.

(84) Remucal, C. K.; McNeill, K. Photosensitized amino acid degradation in the presence of riboflavin and its derivatives. *Environ. Sci. Technol.* **2011**, *45* (12), 5230–5237.